

# Tuning Light Absorption in Pyrene: Synthesis and Substitution Effects of Regioisomeric Donor–Acceptor Chromophores

Samantha N. Keller, Nicole L. Veltri, and Todd C. Sutherland\*

Department of Chemistry, University of Calgary, 2500 University Drive NW,  
T2N 1N4 Calgary, Canada

todd.sutherland@ucalgary.ca

Received July 31, 2013

## ABSTRACT



Three isomeric donor–acceptor (DA) chromophores based on pyrene were synthesized to study the effects of substitution pattern on intra-molecular charge-transfer absorption through pyrene. These chromophores are nonfluorescent and absorb light in the long-wavelength region approaching 700 nm, making them promising light-harvesters. Their optical properties depend greatly on the substitution pattern of the donor, but their electrochemical properties are relatively unaffected.

Pyrene is a well-known photochemist's molecule, and for many years it has been utilized in a variety of applications such as sensing and biological imaging.<sup>1–3</sup> Modern synthetic methods now provide access to nonsymmetric substitution patterns on pyrene that were previously difficult to achieve, thus enabling pyrene to be utilized as a building block for organic electronic materials.<sup>4–7</sup> The optoelectronic properties of such materials are often tuned using a combination of electron-rich (donor, D) and electron-poor (acceptor, A) substituents. However, there

are few examples<sup>8–10</sup> of this “push–pull” strategy employed on pyrene and none that investigate the effect of the regiochemical relationship between donor and acceptor. With this in mind, we have synthesized a series of three isomeric pyrene-based “push–pull” chromophores in order to study the regiochemical effects on their photo-physical and electrochemical properties. An  $\alpha$ -diketone serves as the acceptor, fixed in the pyrene k-region, while the positions of the donor substituents,  $N,N$ -didodecyl-4-ethynylaniline, are varied.

$N,N$ -Didodecyl-4-ethynylaniline and pyrene-4,5-diketone **1** were synthesized according to known methods.<sup>11,12</sup> In order to perform Sonogashira cross-coupling to attach the donor aniline groups to the central diketone acceptor, a series of dibrominated pyrene diketones were prepared

(1) Karuppannan, S.; Chambron, J.-C. *Chem.—Asian J.* **2011**, *6*, 964–984.

(2) Manandhar, E.; Wallace, K. J. *Inorg. Chim. Acta* **2012**, *381*, 15–43.

(3) Wang, G.; Geng, J.; Zhang, X.; Cai, L.; Ding, D.; Li, K.; Wang, L.; Lai, Y.-H.; Liu, B. *Polym. Chem.* **2012**, *3*, 2464–2470.

(4) Zöphel, L.; Beckmann, D.; Enkelmann, V.; Chercka, D.; Rieger, R.; Mullen, K. *Chem. Commun.* **2011**, *47*, 6960–6962.

(5) Kawano, S.-i.; Baumgarten, M.; Chercka, D.; Enkelmann, V.; Mullen, K. *Chem. Commun.* **2013**, *49*, 5058–5060.

(6) Figueira-Duarte, T. M.; Müllen, K. *Chem. Rev.* **2011**, *111*, 7260–7314.

(7) Zöphel, L.; Enkelmann, V.; Rieger, R.; Müllen, K. *Org. Lett.* **2011**, *13*, 4506–4509.

(8) Ottonelli, M.; Piccardo, M.; Duce, D.; Thea, S.; Dellepiane, G. *J. Phys. Chem. A* **2011**, *116*, 611–630.

(9) Sung, J.; Kim, P.; Lee, Y. O.; Kim, J. S.; Kim, D. *J. Phys. Chem. Lett.* **2011**, *2*, 818–823.

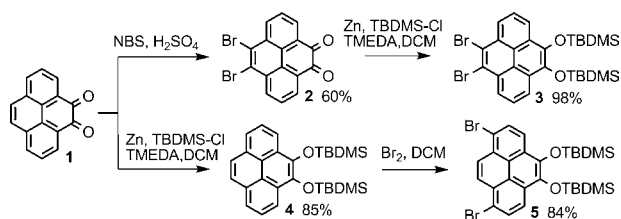
(10) Zöphel, L.; Enkelmann, V.; Müllen, K. *Org. Lett.* **2013**, *15*, 804–807.

(11) Tykwinski, R. R.; Schreiber, M.; Carlón, R. P.; Diederich, F.; Gramlich, V. *Helv. Chim. Acta* **1996**, *79*, 2249–2281.

(12) Hu, J.; Zhang, D.; Harris, F. W. *J. Org. Chem.* **2004**, *70*, 707–708.

divergently from pyrene-4,5-diketone **1**; the diketone moiety is reduced and protected to facilitate the Pd-catalyzed coupling reactions, which are known to be hindered by the presence of the  $\alpha$ -diketone.<sup>13,14</sup> As shown in Scheme 1, the 4,5-dibromo-9,10-pyrene diketone **2** was produced by regioselective bromination of **1** according to the procedure by Mullen et al.<sup>4</sup> Reduction of **2** with zinc and in situ protection with the tertbutyldimethylsilyl (TBDMS) chloride afforded the protected 4,5-dibromo isomer **3**.<sup>15</sup> Reversing the order of reduction and bromination of **1** resulted in bis silyl-protected 1,8-dibromo isomer **5**.

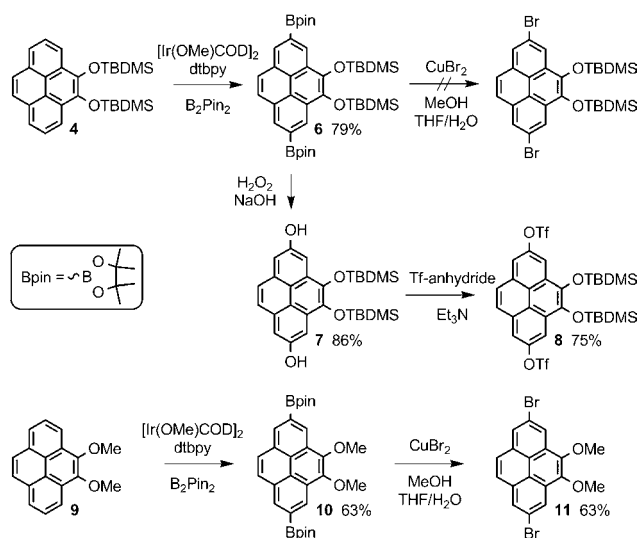
**Scheme 1.** Synthesis of 4,5-Dibromo- and 1,8-Dibromo-Protected Diketone Isomers for Cross-Coupling



Synthesis of the more elusive 2,7-dibromo isomer began by subjecting bis-silyl **4** to the iridium-catalyzed regioselective borylation developed by Marder et al.<sup>16,17</sup> resulting in bis-pinacol borane **6**, as shown in Scheme 2. To our knowledge, this is the first report of this reaction on a substituted pyrene, and it is important to note that the regioselectivity is maintained at the 2,7 positions. However, continuing with Marder's method failed to produce the dibrominated compound and instead resulted in the deprotection of the TBDMS groups.<sup>18</sup> A second route was attempted from bis-pinacol borane **6** to form the protected 2,7-dihydroxypyrene **7**, which was subsequently triflated to give **8**. However, poor yields were obtained in the Sonogashira cross-coupling reaction between bis-triflate **8** and *N,N*-didodecyl-4-ethynylaniline. We then surmised that less steric bulk might aid the cross-coupling step and the TBDMS ether protecting groups were replaced with methyl ethers. The route began with 4,5-dimethoxypyrene **9** (produced according to the method of Bodwell et al.<sup>19</sup>) that was borylated to give **10** and finally brominated to obtain the protected 2,7-dibromo isomer **11**.

With the three isomers in hand, Sonogashira cross-coupling reactions was carried out with *N,N*-didodecyl-4-ethynylaniline **12** to obtain protected pyrene isomers **13–15**, as shown in Scheme 3. The three protected pyrenes

**Scheme 2.** Synthetic Strategies Used To Access the Protected 2,7-Dibromo Isomer (**11**)



were subsequently deprotected and reoxidized to form the final regioisomeric D–A–D chromophores **16** to **18**.

**Scheme 3.** Cross-Coupling, Deprotection, and Oxidation To Afford Regioisomeric Pyrene D–A Chromophores

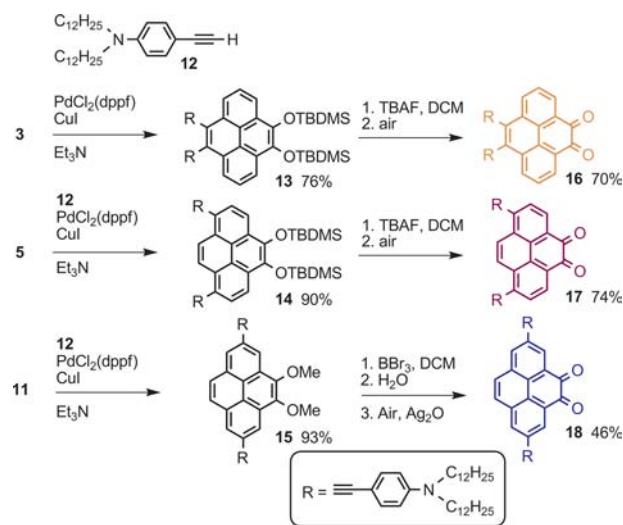


Figure 1 shows the absorption spectra of diketones **16** to **18** in chloroform at  $10^{-6}$  M concentrations. Diketone **16** shows absorptions starting at 500 nm, which is consistent with a charge transfer (CT) band centered at 470 nm, as was observed on similarly substituted pyrene D–A compounds by Müllen et al.<sup>10</sup> The CT absorption band of **17** is of similar intensity as **16**, but is strongly red-shifted with a broad band centered at 570 nm and extending to over 700 nm. The CT band of **18** is the furthest red-shifted (575 nm peak), but the least intense of the three isomers. However, diketone **18** has an extremely strong  $\pi$ – $\pi^*$  transition at 385 nm with a molar absorptivity nearing

(13) More, S.; Bhosale, R.; Choudhary, S.; Mateo-Alonso, A. *Org. Lett.* **2012**, *14*, 4170–4173.

(14) Estrada, L. A.; Neckers, D. C. *J. Org. Chem.* **2009**, *74*, 8484–8487.

(15) Ciszek, J. W.; Tour, J. M. *Tetrahedron Lett.* **2004**, *45*, 2801–2803.

(16) Coventry, D. N.; Batsanov, A. S.; Goeta, A. E.; Howard, J. A. K.; Marder, T. B.; Perutz, R. N. *Chem. Commun.* **2005**, 2172–2174.

(17) Crawford, A. G.; Liu, Z.; Mkhalid, I. A. I.; Thibault, M.-H.; Schwarz, N.; Alcaraz, G.; Steffen, A.; Collings, J. C.; Batsanov, A. S.; Howard, J. A. K.; Marder, T. B. *Chem.—Eur. J.* **2012**, *18*, 5022–5035.

(18) Tan, Z. P.; Wang, L.; Wang, J. B. *Chin. Chem. Lett.* **2000**, *11*, 753–756.

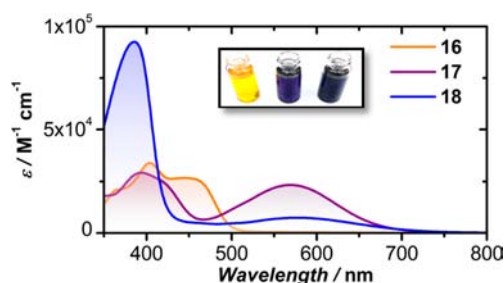
(19) Venkataramana, G.; Dongare, P.; Dawe, L. N.; Thompson, D. W.; Zhao, Y.; Bodwell, G. J. *Org. Lett.* **2011**, *13*, 2240–2243.

**Table 1.** Optical, Electrochemical, and Calculated Properties of Pyrene Chromophores **16–18**

	$\lambda_{\text{abs}}^a$ (nm)	$\epsilon$ ( $\text{M}^{-1} \text{cm}^{-1}$ )	$\lambda_{\text{onset}}^a$ (nm)	$E_{\text{opt}}^b$ (eV)	$E_{\text{ox(DPV)}}^c$ (V)	$E_{\text{red(DPV)}}^c$ (V)	$E_{\text{ox}} - E_{\text{red}}^c$ (eV)	$E_{\text{LUMO-HOMO}}^{\text{DFT}}^d$ (eV)	$\mu_{\text{DFT}}^d$ (D)
<b>16</b>	450	26600	500	2.3	0.29	−1.07	1.4	2.04	15
<b>17</b>	570	23000	700	1.7	0.40	−1.11	1.5	2.34	16
<b>18</b>	575	7400	700	1.6	0.33	−1.04	1.4	2.06	6

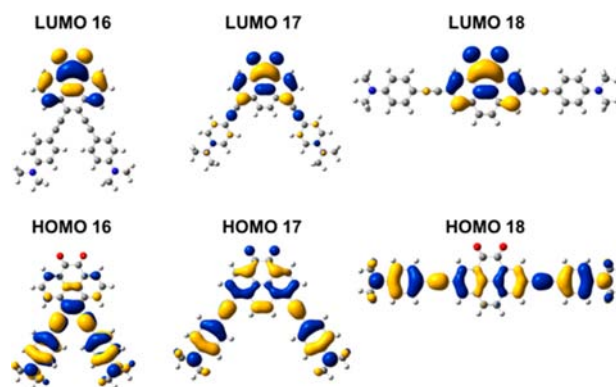
<sup>a</sup> Measured in  $\text{CHCl}_3$ . <sup>b</sup> Calculated from  $\lambda_{\text{onset}}$ . <sup>c</sup> CV and DPV potentials are referenced to an internal ferrocene/ferricenium redox probe in  $\text{CH}_2\text{Cl}_2$  containing 0.05 M  $(n\text{Bu})_4\text{PF}_6$  with a Pt button working electrode, a Ag wire quasi reference electrode, and a Pt wire counter electrode at  $20 \text{ mV} \cdot \text{s}^{-1}$ . <sup>d</sup> B3LYP/6-31G+(d) using Gaussian09.

$10^5 \text{ M}^{-1} \cdot \text{cm}^{-1}$ . Chloroform solutions of **16**, **17**, and **18** are yellow, purple, and blue, as shown by the inset of Figure 1. The absorption profile of diketones **16** to **18** did not change between  $10^{-5}$  and  $10^{-6} \text{ M}$  chloroform solutions, indicating little aggregation or dimerization effects that are commonly observed in pyrene.<sup>20</sup> None of the diketones displayed fluorescence, although their respective precursors **13–15** were highly fluorescent (see the Supporting Information, Figure S1).

**Figure 1.** UV/vis absorption spectra of diketones **16** (orange), **17** (purple), and **18** (blue) in  $\text{CHCl}_3$ . (Inset: photo of **16–18** left to right in  $\text{CHCl}_3$ .)

Insight into the large variation in optical properties between the isomers was gained by DFT calculations. Optimized structures (B3LYP/6-31G+(d)) and MOs of truncated models (dodecyl chains are replaced by Me groups) of **16–18** are shown in Figure 2. Optimized model diketone **16** shows the two anilines twisted out-of-plane with respect to the pyrene core, whereas optimized model diketones **17** and **18** show aniline rings that are coplanar with the pyrene core. The HOMO of **16** is localized to the ethynylaniline fragments, in contrast to the HOMOs of **17** and **18**, which have MO coefficients that span both donor and acceptor portions of the molecule. The LUMOs of all three diketones have near-identical coefficients and lie at similar energy, residing on the electron-poor, acceptor pyrene core. The nonplanar anilines in **16** and aniline-localized MOs supports a typical donor–acceptor model of the intramolecular CT band.<sup>21,22</sup> Conversely, the

coplanarity of the anilines with pyrene in both **17** and **18** suggests a donor–acceptor system whereby the donor component spans both the anilines and the pyrene, which is consistent with the HOMO coefficients. Because of the delocalized HOMOs in **17** and **18**, the “donor” portion of the molecules is enhanced leading to a large red-shift in the CT band. The intensity of the CT bands of **16** and **17** are comparable, but the CT band of pyrene **18** is much attenuated. The CT band intensity is attributed to the differences in transition dipole moments. Both diketones **16** and **17** possess calculated ground-state dipoles of 15 and 16 D, whereas pyrene **18** has a much smaller ground-state dipole of 6 D, leading to a smaller transition dipole. As shown in Table 1, the DFT-calculated values for the HOMO–LUMO energy gaps of **16–18** are overestimated and do not reflect the trend shown in the optical data. However, for highly delocalized CT states such as these and other organic dyes and light-harvesters, it is common to observe this poor reproducibility between theoretical and experimental values using DFT methods.<sup>23–25</sup>

**Figure 2.** DFT-optimized structures and FMO plots of truncated models of diketones **16–18** at the B3LYP/6-31G+(d) level using Gaussian09.

Despite the drastic difference in optical properties between the three isomers, they are electrochemically very

(20) Reynders, P.; Kuehnle, W.; Zachariasse, K. A. *J. Am. Chem. Soc.* **1990**, *112*, 3929–3939.

(21) Sumalekshmy, S.; Gopidas, K. R. *J. Phys. Chem. B* **2004**, *108*, 3705–3712.

(22) Sumalekshmy, S.; Gopidas, K. R. *New J. Chem.* **2005**, *29*, 325–331.

(23) Reimers, J. R.; Cai, Z.-L.; Bilić, A.; Hush, N. S. *Ann. N.Y. Acad. Sci.* **2003**, *1006*, 235–251.

(24) Dev, P.; Agrawal, S.; English, N. J. *J. Chem. Phys.* **2012**, *136*, 224301–11.

(25) Karolewski, A.; Stein, T.; Baer, R.; Kummel, S. *J. Chem. Phys.* **2011**, *134*, 151101–4.

similar. The cyclic voltammograms (CVs) and differential pulse voltammograms (DPVs) are shown in Figure S2 (Supporting Information), and the redox potentials, referenced to ferrocene, are listed in Table 1. In the oxidation region, diketones **16–18** show a typical irreversible aniline-type oxidation<sup>26</sup> between 0.3 and 0.4 V, and application of higher oxidation potentials did not result in electrochemical peaks, but rather broad featureless decomposition. For comparison, the *N,N*-didodecyl-4-ethynylaniline precursor has an oxidation potential of 0.42 V (vs Fc/Fc<sup>+</sup>) under identical electrochemical conditions. Diketones **16** and **18** are slightly more difficult to oxidize than pyrene **17** because pyrene **17** has a stabilized HOMO energy level due to enhanced conjugation relative to **16** and **18**. The enhanced conjugation of **17** is supported by FTIR measurements that show both lower energy alkyne and carbonyl stretching frequencies. Diketones **16**, **17**, and **18** each show reversible reduction reactions at approximately  $-1.1$  V. Pyrene diketone **1** has a similar reduction potential of  $-1.15$  V (vs Fc/Fc<sup>+</sup>). Overall, the electrochemical redox reactions are in general agreement with the redox potentials of the isolated donor and acceptor components, implying minimal electronic perturbation of the ground-state molecules and electrochemically diketones **16–18** behave as isolated electrophores. There is a large discrepancy between the electrochemical and optical HOMO–LUMO energy gaps, which is attributed to the difference between ground-state electron transfer reaction that occurs at a Pt surface and photoexcitation.

Spectroelectrochemical (SEC) UV/vis absorption and FTIR spectra of the reduced diketones are shown in Figure 3 and Figure S4 (see the Supporting Information), respectively. Upon reduction, the pyrene diketones are reduced to the pyrene dioxide dianions, which convert the DAD system to a DDD system commensurate with a collapse of the CT band, which is observed clearly in Figure 3. The disappearance of the intense CT band in pyrene **17** is a promising feature for electrochromic applications. The SEC FTIR spectra of **17** and **18** show the decrease in the intensity of the carbonyl and alkyne stretching frequencies, consistent with the carbonyl reduction and aromatization of pyrene.

(26) Hambitzer, G.; Heitbaum, J.; Stassen, I. *J. Electroanal. Chem.* **1998**, *447*, 117–124.

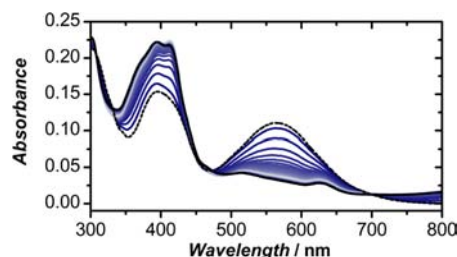


**Figure 3.** UV–vis absorption spectra of **17** as a function of applied potential ( $-600$  mV vs Ag wire quasi reference) taken at 1 min intervals. Initial spectra (0 V applied) are dotted black lines, and final spectra are the solid black lines with blue lines representing the spectral evolution.

In summary, we present a poly functionalization synthetic strategy to access three regioisomers of a “push–pull” pyrene-based chromophore. Despite the similar molecular makeup of the three isomers, their optical absorption properties vastly differ owing to the efficiency in absorbing photons through the CT band. Electrochemically, the three compounds behave similarly, suggesting independence of the electrophoric units in the ground state. DFT calculations support the ground-state structure and provide insight into the observed optical transitions. In addition to being light-harvesters, these compounds also display electrochromic behavior.

**Acknowledgment.** We thank the Natural Sciences and Engineering Research Council (NSERC) of Canada for financial support. S.N.K. acknowledges scholarship support from the NSERC CGS program and Alberta Innovates. N.L.V. thanks the University of Calgary for support through the Program for Undergrad Research Experience (PURE). We thank West Grid and Compute Canada for computational resources.

**Supporting Information Available.** Experimental details; <sup>1</sup>H and <sup>13</sup>CNMR spectra of products; fluorescence spectra of **13–15**; electrochemical voltammograms, FTIR, SEC-FTIR, and SEC-UV–vis of **16–18**; computational details. This material is available free of charge via the Internet at <http://pubs.acs.org>.

The authors declare no competing financial interest.